Journal of VLSI Design Tools and Technology
Volume 2, Issue (1-3), Compilation 2012

STM JOURNALS

System Level Modeling of ISMB Quadrature Transceiver

Rupam Goswami[1], Prashant Singh[1], Narendra Bahadur Singh[2]*
[1]Graduate Students, [2]Chief Scientist, MEMS, MS & RF ICs Design Semiconductor Devices Area
Central Electronics Engineering Research Institue (CSIR-CEERI) Pilani, Rajasthan-333031,India

ABSTRACT

In this paper, a new ISMB quadrature transceiver system-level design architecture is presented along with its referenced mathematical models and these were verified using state-of-the-art system modeling tools. Unlike a K-TEK's receiver, it does not suffer from the timing and template matching problems, and it circumvents processing at high frequencies, thereby reducing the on-chip circuit complexity and power consumption. Hilbert transform has been used at the output of the demodulator for the envelope detection to get the more reliable desired signal that is also the uniqueness in the system. It also presents parallel approach to use a band-pass filter at the output of the demodulator to eliminate the d.c. component to get the desired signal. Matlab coding and Simulink system modeling were parallel done before the design of monolithic integrated circuit using CMOS technology to transfer the similar function on silicon and the objective is completed for most of the blocks. The system-level simulation, presented in this paper, shows the functional behavior of the proposed transceiver.

***Keywords**: Industrial, scientific and medical radio band, narrowband interference, quadrature downconversion receiver, Hilbert transform, convolution, FFT, DFT, Chebyshev filter, Matlab, Simulink*

****Author for Correspondence*** E-mail: nbs44254@gmail.com

1. INTRODUCTION

The industrial, scientific and medical (ISM) radio band technology has gained much interest during the last few years as a potential candidate for future wireless short-range data communication [1]. Recently, these bands have also been shared with license-free error-tolerant communications applications such as wireless LANs, Bluetooth and cordless phones in the 915 MHz, 2.45 GHz, and 2.483 GHz and 5.8 GHz bands. The ISM band [14] is also widely used for RFID application. Frequency band used in this paper is 2.4 GHz (ISM) [2] unlicensed band. Due to its almost global availability, it constitutes a popular frequency band suitable for low-cost radios. Due to its large bandwidth, ISMB has the promise of high data rates.

In order to improve spectral efficiency and information capacity, phase modulation techniques such as BPSK and QPSK are used. QPSK involves phase-only modulation and provides a good balance between information capacity, ease of implementation and bit-error rate. QPSK modulation permits twice the amount of information to be carried within the same bandwidth as BPSK with little additional complexity. Thus, it is used in ISM bands. Traditional passive QPSK modulators generally employ a pair of balanced BPSK modulators, which are then typically power-combined using a Wilkinson or Lange coupler [3, 4]. Moreover, there has been a definite drive to achieve direct modulation in order to reduce RF front-end complexity through removal of IF stages. While many high-performance topologies have previously been presented, the presence of filters in these

topologies adds complexity and prevents direct scaling to millimeter wave frequencies.

Figures of merit for QPSK modulators include bandwidth, insertion loss, EVM and power consumption [5]. The system presented in this paper is superior to previous implementations on a combination of certain parameters. The bandwidth of the QPSK modulator determines the maximum data rates that can be transmitted. The modulator presented here allows operation over nearly an octave bandwidth.

The most commonly used modulation scheme for wireless and cellular systems is quadrature phase shift keying (QPSK). It is because it does not suffer from BER degradation while the bandwidth efficiency is increased. The absence of high-power-consumption active devices limits the power consumption of the designed modulator to less than 10 µW [5]. This paper suggests a new QPSK receiver architecture without using the filter advantages with respect to the other receiver. It deals with interference rejection without filtering and avoids high frequency on-chip processing by using frequency conversion.

2. PROPOSED QPSK RECEIVER

The proposed receiver architecture is shown in Figure 1. QPSK can be stated as a method for transmitting digital information across an analog channel. The receiver consist of two coherent detector supplied with the same input signal, namely, the incoming DSB-SC wave $[1 + K_a.m(t)] * (A_c cos(\omega_c t))$, but with individual local oscillator signals that in phase quadrature with respect to each other.. The frequency of the local oscillator is adjusted to be the same as the carrier frequency f_c. The detector in the upper path is referred to as the in-phase coherent detector or I-channel, that in the lower path is referred to as the qudrature-phase coherent detector or Q-channel. These two detectors are coupled together to form negative feedback system design in such a way as to maintain the local oscillator synchronous with the carrier wave [7].

In the transmitted reference scheme, two pulses per symbol are sent with a certain chosen delay τ_d [8], [9] between them. After mixing the signal, one pulse are delayed by τ_d (almost 90^0) and connected to the multiplier. To obtain the demodulated signal both delaying I & Q-signal are adding by an adder circuit and apply to the Envelope detector see in Figure 1. [6].

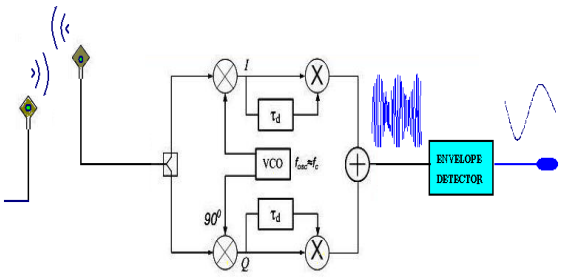

Fig. 1: *ISMB Quadrature Down Conversion Receiver [6].*

A baseband cosine signal is mixed with the carrier of same frequency range of receiver

and following the same analysis. As can be seen in Figure 1, a modulated signal is obtained after adder presented in Section 3. Thus, if the envelope detector is neglected, then Figure 1 is used as a modulator. The parameters of demodulator block are shown in Table I.

Table I: *Simulation Parameters of Demodulator*

Specification	Simulated
Base band frequency	400 MHz
Carrier frequency	2.45 GHz(ISM)
Time delay	0.104 ns
Modulation index	0.4

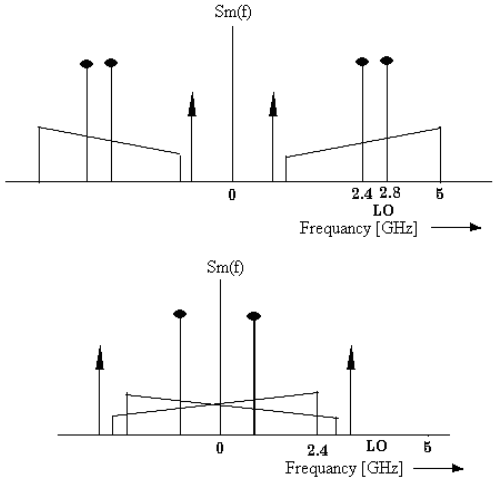

Fig. 2: *The ISMB Spectrum of Narrowband Interferers at 2.4 GHz and 2.8 GHz (a) Before Downconversion (b) After Downconversion* [10].

3.1. Time Domain Analysis

Because ISM band systems rely on timing information, we will use a time-domain analysis [6] throughout the remainder of this paper. A conventional AM wave can be represented by:

$$S_m = [1 + K_a.m(t)] * (A_c \cos(\omega_c t)) \quad (1)$$

where $m(t) = A_m \cos(\omega_s t)$ represent a base band signal. A_c Is the carrier amplitude envelope, ω_c is the carrier frequency. This description is commonly used for carrier-based signals but can also be applied to pulse-based signals as long as they have a band pass spectrum.

Now, consider a situation where two pulses of equal sign are transmitted. For the moment, assume that we have only the upper path of the circuit shown in Figure 1. This path is denoted here as the in-phase path.

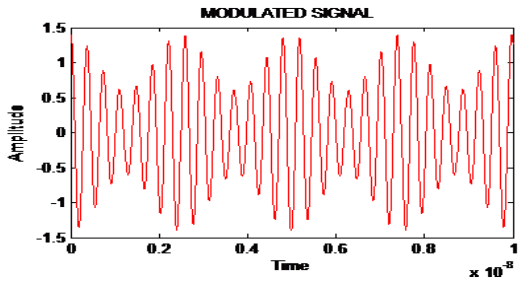

Fig. 3: *A Typical Modulated Wave.*

After mixing with a modulated signal (Figure 3) of angular frequency and taking normalized amplitude as one, then using Eq. (1), we obtain the signal for the upper path:

$I = S_m(t)*(A_c\cos(\omega_c t + \text{ø}(t)))$ (2)

$\text{ø}(t)$ is the phase modulation, denoted by "0".

After calculating Eq. (2), it is expressed as,

$I = ½A_c^2$

$[1 + \cos(2\omega_c t) + K_a\cos(\omega_s t) + ½K_a\{\cos(2\omega_c + \omega_s)t + \cos(2\omega_c - \omega_s)t\}]$ (3)

After delaying this pulse in [6], the delayed path:

$I_d = ½A_c^2[1 + \cos(2\omega_c(t-\tau_d))+K_a\cos(\omega_s(t-\tau_d)) + ½K_a\{\cos(2\omega_c + \omega_s)(t-\tau_d) + \cos(2\omega_c-\omega_s)(t-\tau_d)\}]$ (4)

To ease the analysis, a change of variable is made by letting $I_d = ½A_c^2$

$[1 + \cos(2\omega_c t') + K_a\cos(\omega_s t') + ½K_a\{\cos(2\omega_c + \omega_s)t' + \cos(2\omega_c-\omega_s)t'\}]$ (5)

This is the signal in the delayed path before the multiplier.

If we multiply the signal in the delayed path and original output of the mixer, then we get the signal of the upper path before the adder seen in Sec. 3. Mathematically, it is written as,

I Channel Path Signal = $I * I_d$ (6)

3.2. The Quadrature Path

The previous analysis assumed perfect synchronization between the oscillator and the "pulse carrier." In reality, this is not the case. Unless the oscillator is being locked onto the incoming signal, there is always a relative phase between the oscillator and the "pulse carrier." Denoting this relative phase,

$\emptyset(t)=\frac{\pi}{2}$ (7)

This means that in Eq. (2) $\omega_c t$ has to be replaced by $\omega_c t + \emptyset(t)$, thus Eq. (2) can be written as,

$Q = S_m(t)*(A_c\cos(\omega_c t + \emptyset(t)))$ (8)

Following the same analysis as in the upper path, it can be found that the signal before adder now equals:

$Q = ½A_c^2[\sin(2\omega_c t) + ½K_a[\sin(2\omega_c + \omega_s)t + \sin(2\omega_c-\omega_s)t]]$ (9)

If (ω_c=ω_m), this means that after envelope detection, the result depends on $\emptyset(t)$. The output can even be zero whereas a positive value was expected. This is a well-known phenomenon in coherent detection. In coherent detection, the oscillator can be locked to the carrier but since in this situation there is a suppressed very weak carrier that is only present when the pulse is present and there is also narrowband interference, this is not possible. A possible solution is to add a similar path but now mixed with a sine (90-phase shift) instead of a cosine and adds the outputs after multiplied with the delayed path, resulting in the architecture shown in Figure 2. This lower path is called the quadrature path; it holds the signal after multiplication with the delayed path and before the adder, i.e.:

$Q = ½A_c^2[\sin(2\omega_c t') + ½K_a[\sin(2\omega_c + \omega_s)t' + \sin(2\omega_c-\omega_s)t']]$ and,

Q-Channel Path Signal = $Q * Q_d$ (10)

After adding Eqs. (6) and (8), we get the required modulated signal – the signal shown in Sec. (3.1).

3.3. Envelope Detection

In signal systems, we often make use of modulated signals. One big problem when we modulate a signal is that its spectrum mirrors itself on both sides of the carrier frequency [9]. Only one of these spectra, or sidebands, is needed to demodulate the signal and therefore we have redundant information. There are different techniques to remove one of the sidebands and thereby create a single sideband signal (SSB). The simplest one is to use a low-

pass filter with the middle of the transition band on the carrier frequency. This technique demands that we have a narrow transition band and a good suppression, which is hard to obtain. Another technique is to use the Hilbert transform where one sideband has been eliminated by adding the signal to itself. Importance to second procedure has been given in this paper because Hilbert transform has the same energy and therefore the energy can be used to measure the calculated accuracy of the approximated Hilbert transform.

3.3.1. Hilbert Transform

The Hilbert transform [11] is considered in three different ways. First one is Cauchy integral in the complex plane, second one is Fourier transform in the frequency domain and in third one ±π/2 phase-shift is used, which is basic property of the Hilbert transform. In this paper, second one is considered. The Hilbert transform $\hat{f}(t)$ of a function f(t) is defined for all t by

$$\hat{f}(t) = \frac{1}{\pi} P \int_{\alpha}^{\alpha} \frac{f(\tau)}{t-\tau} d\tau \qquad (11)$$

when the integral exists.

It is normally not possible to calculate the Hilbert transform as an ordinary improper integral because of the pole at τ = t. However, the P in front of the integral denotes Cauchy principal value which expands the class of function for which the integral definition exists. To derive the discrete Hilbert transform, it needs the definition of the discrete Fourier transforms (DFT) [12], that is

$$F[k] = \sum_{n=0}^{N-1} f[n]\, e^{-i\frac{2\pi}{N}kn}, k = 0,1, \ldots \ldots \ldots N-1 \qquad (12)$$

and the inverse formula,

$$f[n] = \frac{1}{N}\sum_{k=0}^{N-1} F[k] e^{-i\frac{2\pi}{N}kn}, n = 0,1, \ldots \ldots \ldots N-1 \qquad (13)$$

where k is the discrete frequency and n is the discrete time. Note that Eq. (13) defines a periodic function with period N. After expanding Eq. (12) in its real and imaginary parts on both sides, thus

$$F[k] = F_{Re}[k] + iF_{Im}[k] \qquad (14)$$

Thus

$$\sum_{n=0}^{N-1} f[n]\, e^{-i\frac{2\pi}{N}kn} = \sum_{n=0}^{N-1} f[n]\cos\left(\frac{2\pi}{N}kn\right) - i\sum_{n=0}^{N-1} f[n]\sin\left(\frac{2\pi}{N}kn\right) \qquad (15)$$

The real and imaginary terms can be written as,

$$F_{Re}[k] = \sum_{n=0}^{N-1} f[n]\cos\left(\frac{2\pi}{N}kn\right)$$

$$F_{Im}[k] = \sum_{n=0}^{N-1} f[n]\sin\left(\frac{2\pi}{N}kn\right)$$

and it concludes that F_{Im} = 0 when k = 0 and k = N/2. The Hilbert transform of the delta pulse δ(t) gives the Hilbert transformer (1/πt) and the Fourier transform of the Hilbert transformer gives the sign shift function -isgn(ω); that is

$$\delta(t) \overset{H}{\Leftrightarrow} \frac{1}{\pi t} \overset{F}{\Leftrightarrow} -isgn(\omega) \qquad (16)$$

The discrete analog of the Hilbert transformer in Eq. (16) for even N is therefore given by,

$$H[k] = -isgn\left(\frac{N}{2} - k\right) sgn(k) \qquad (17)$$

and H[k] can be written in the form,

The discrete inverse Fourier transform of the discrete Hilbert transformer in Eq. (17) gives the discrete impulse response in the time domain, for even N:

$$h[n] = \frac{2}{N}\sum_{n=0}^{\frac{N}{2}-1} \sin\left(\frac{2\pi}{N}kn\right)$$

and h[n] can be expressed in closed form as,

$$h[n] = \frac{2}{N} sin^2 \frac{\pi n}{2} cot \frac{\pi n}{N}$$

The function is given by the cotangent function with every second sample (n = 0,2,4….) erased by $sin^2(n)$; see Figures 4a and 4b.

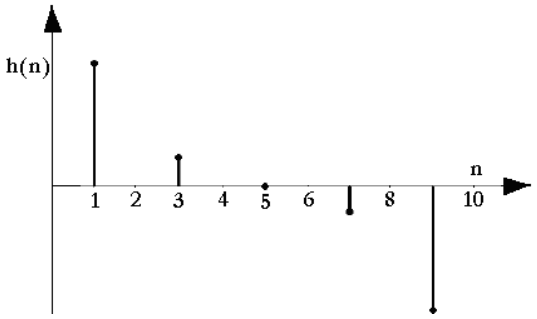

Fig. 4a: *The Discrete Impulse Response of the Hilbert Transform for Even N (N = 10)* [11].

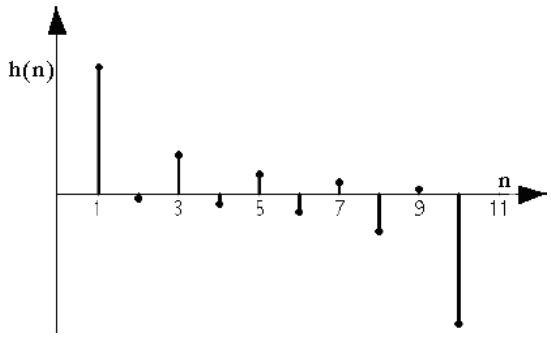

Fig. 4b: *The Discrete Impulse Response of the Hilbert Transform for Odd N (N = 11)* [11].

The same derivation for Odd *N* we get

$$h[n] = \frac{2}{N} \sum_{n=0}^{\frac{N-1}{2}} \sin\left(\frac{2\pi}{N} kn\right)$$

Where the closed form of h[n] can be expressed as

$$h[n] = \frac{1}{N} \left(\cot\left(\frac{\pi n}{N}\right) - \frac{\cos(\pi n)}{sin\frac{(\pi n)}{N}}\right)$$

Therefore it occludes that it does not have the same cancellation for odd N (4.b) as for even N (4.a), instead h[n] is changing sign by odd and even values of n, shown in fig.4a &b.

The discrete Hilbert transform of the sequence $\hat{f}(n)$ is defined by convolution on form

$$\hat{f}(n) = \sum_{m=0}^{N-1} h[n-m] f[m] \quad (18)$$

If one instead chooses to use the DFT algorithm [11] then following relations exist,

$$f[n] \overset{DFT}{\Longrightarrow} F[k] \overset{DFT}{\Longrightarrow} \hat{F}[k] =$$

$$-isgn\left(\frac{N}{2} - k\right) sgn(k) F[k] \overset{DFT^{-1}}{\Longrightarrow} \hat{f}(n) \quad (19)$$

where DFT denotes the discrete Fourier transform, DHT denotes the discrete Hilbert transform and DFT^{-1} denotes the discrete inverse Fourier transform.

The discrete convolution algorithm [Eq. (18)] is faster than the DFT algorithm [Eq. (19)] because it involves only a single summation. The accuracy of the discrete Fourier transform when applied to continuous signals depends on how many samples happen in our calculation. It is important that the sample frequency is higher than double the signal frequency, which is the Nyquist frequency.

3.4. Power Calculations

Since, signal m(*t*) is considered, where *t* is an index of the sample number, we define the instantaneous power [13] of the signal as,

$$P_{ins} = m^2(t) \quad (20)$$

Average power is more useful quantity, which is simply the average of the instantaneous power of every sample in the signal. For signal m(*t*), of *N* samples, average power is represented as,

$$P_{ave} = \frac{1}{N} \sum_{t=1}^{N} m^2(t) \quad (21)$$

3.5. Simulation Results

To verify the functional behavior of the proposed receiver, the system was simulated in Matlab/Simulink. First, the ideal situation was simulated. The initial phase of the oscillator was set to zero; the delay in the receiver matched the delay between the pulses in the transmitter (equal to the pulse repetition time) and the oscillator period was a perfect integer of this delay; no amplitude mismatch was present in the two paths and the oscillator signals had a perfect quadrature relation [7]; the oscillator amplitude in both paths was set to one. The absolute value of the output in this ideal case serves as the reference value, as from the analysis in Sec. 2, it followed that any mismatch appearing in the system will degrade the output value. All subsequent results will be normalized to this value to show the performance loss. Figure 5 shows the simulation plot of the proposed architecture.

A modulated signal of 5 mV was given as an input to the receiver shown in Figure 5b. The demodulated signal is in the 5 mV range and no phase change occurred compared to the input. The magnitude of the demodulated signal as a function of time is presented in the Figure 5c. The signal contains no negative term so there is no chance of performance degradation. The delay using the mixer output is approximately 0.104 ns. Mismatching this value, a valuable change occurred at the output level. The power consumption of the designed demodulator is less than 10 µW.

Secondly, Figure 5.1 shows that the modulator's signal magnitude is also in 0.4 mV range. Therefore, we conclude that the transceiver system lost only 0.1 mV amplitude for transmitting and receiving the signal. The power consumption of the designed modulator is 8.5 µW [5].

Thirdly, the demodulated signal neglecting d.c. component. If the dc component is removed from the I-Q summation signal, then envelope detector is not required. The demodulated signal is received without envelope detector. It is also clear that in a receiver for negligible interference, envelope detector is not desired. It emphasizes circuit simplicity and low power consumption of the system.

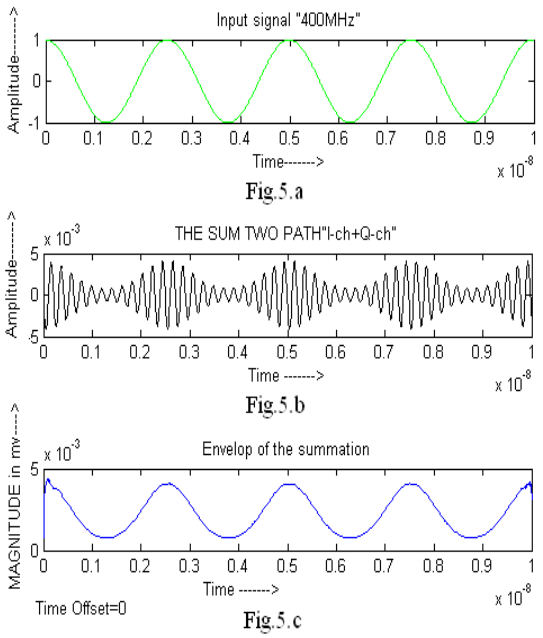

Fig. 5: *The Demodulator's (a) Base Band Signal (b) Summation of I and Q-Channels (c) Envelope of the I + Q Signals Respectively.*

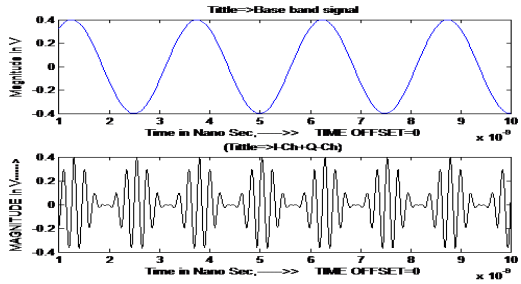

Fig. 5.1: *The Modulator Baseband Signal and Modulated Signal.*

3. SYSTEMS DESIGN USING SIMULINK

Simulink is a powerful simulation and modeling tool for use within the MATLAB environment. It is able to simulate both mechanical and electrical systems, but during this investigation, it only concerned with the electronic systems applicable to communications. The systems are designed using block diagrams where the user can manipulate blocks and connect them as required. The scope of the paper is to present the complete step-wise response at each stage of the QPSK architecture using Simulink modeling which were never presented earlier. It gives the complete inside details of the QPSK system.

4.1. System Architectures

The above demodulator block is now modeled in Simulink. The block of demodulator used in system simulation is shown in Figure 6. In this paper, 400 Mhz of message signal is considered and 2.4 Ghz as a carrier. To understand the operation of this receiver, suppose the local oscillator signal is of the same phase as the carrier wave $A_c \cos(\omega_c t)$ used to generate the incoming DSB-Sc wave. Under these conditions, it is found that the I-Channel output contains the desired demodulated signal m (t), whereas the Q-channel output is zero due to the quadrature null effect of the Q-channel. If the local oscillator phase drifts from its proper value by a small angle ø degree then there will be some signal appearing at the Q-channel output, which is proportional to the sinø ~ ø for small ø. Now, the Q-channel output will have the same polarity as happens in the I-channel output.

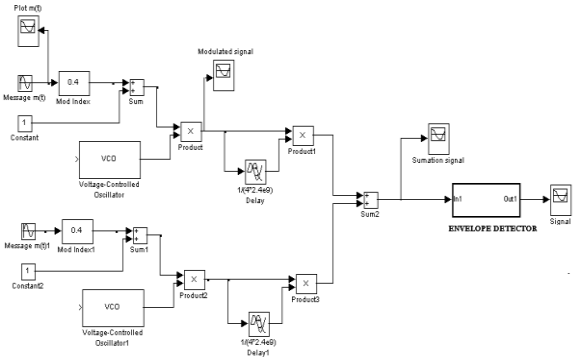

Fig. 6: *The block of the Demodulator QPSK.*

The envelope detector block is a code resume subsystem. It contains a diode as a switch and Chebyshev lowpass filter type 2 which are connected in series. The chebyshev lowpass filter consists of the following properties:

Filter order: 4Stop band edge frequency: 2.8 Ghz Stop band attenuation: 60 dB

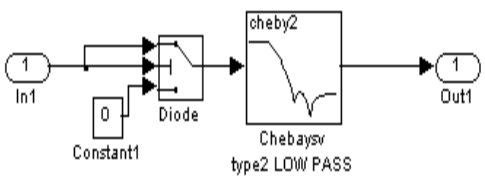

Fig. 6.1: *Envelope Detector.*

Now the same block as in Figure 6.2 is designed using DSB-AM modulation block in place of the coherent detector.

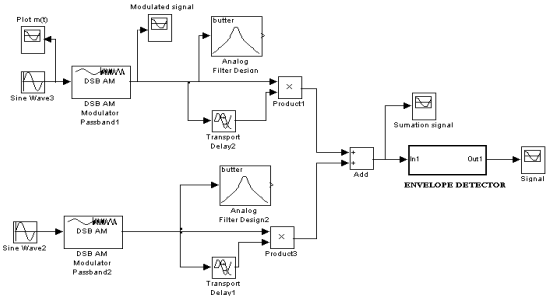

Fig. 6.2: *QPSK Demodulator Using DSB-AM.*

4.2. QPSK Modulator

Since, demodulation is just a reverse process of modulation, here the system architecture is described in Simulink for the modulation with modulation index 0.4. This modulated signal is used as the input to the demodulator as shown in Figure 7.

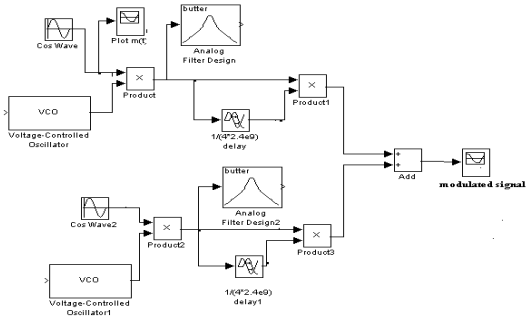

Fig. 7: *QPSK Modulator.*

4.3. Simulation Results

To verify the functional behavior of the proposed receiver, the system was simulated in Matlab/Simulink, assuming filters to be absent. These assumptions are justified as negligible interference.

The simulation result of the transceiver system for demodulator block is shown in Figure 8 and for modulator block it is shown in Figure 3. Here, time offset is zero and time axis varies from 0 to 10 ns.

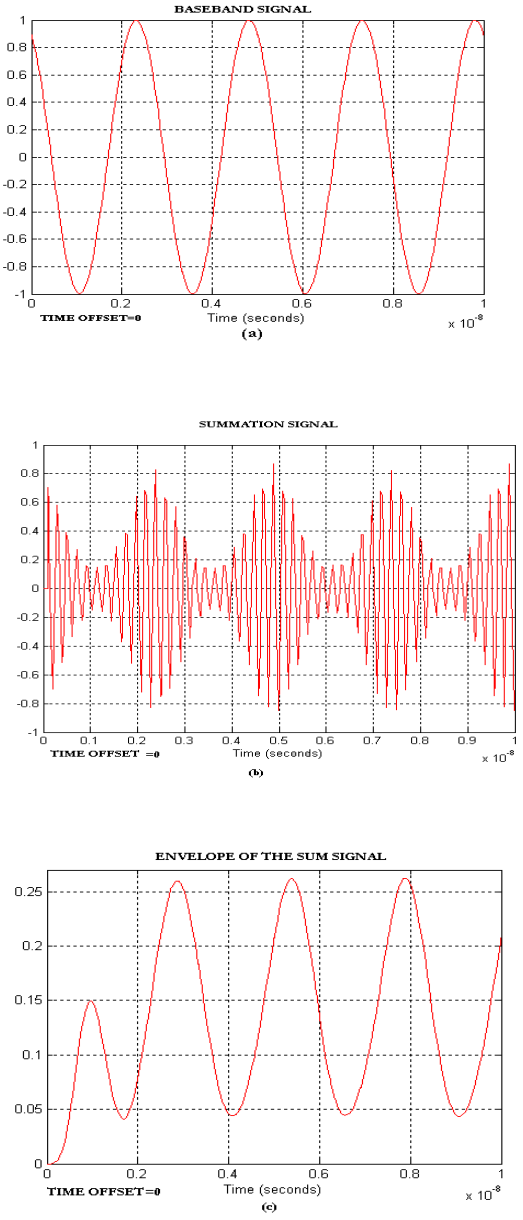

Fig. 8: *Demodulator's Response (a) Message signal (b) Summation (I + Q) signal and (c) Envelope of the sum (I + Q) Signal.*

4. CONCLUSIONS

A new ISMB receiver architecture has been presented in the paper that includes Hilbert

transform to get the demodulated signal for the more reliable behavior of the demodulator. Demodulated signal can also be received at the output of the demodulator after eliminating d.c. component using band-pass filter as presented in the paper. It avoids high-frequency processing, allowing for reduction of the on-chip circuit complexity and power consumption less than 10 µW for the simulated behavior. Assuming component matching that can be readily achieved in today's IC technologies, Matlab/Simulink simulation shows only 0.5 mV error occurred compared to input. Hence it is concluded that power accuracy is almost 95%. Performance degradation due to the amplitude mismatch and phase error is negligible but after change in the angle of delay compared to 90, it gives some degradation at the output.

REFERENCES

1. Nada Golmie and Frederic Mouveaux. *Proceedings of IEEE International Conference on Communications, ICC 2000*. New Orleans, LA. June 2000. 3. 1563–1567p.
2. L. Yang and G. B. Giannakis. *IEEE Signal Processing Magazine*. November 2004. 21(76). 26-54p.
3. S. Yi, A. P. Freundorfer and D. Sawatzky. *Canadian Conference on Electrical and Computer Engineering*. May 2005. 1882-1885p.
4. S. Kumar and G. Wells. *Electronics Letters*. 26(14). July 1990. 961-962p.
5. T. Pochiraju, V. F. *Fuscom. Microwave Symposium Digest.* 15-20 June 2008. IEEE MTT-S International.
6. Simon Lee, S. Bagga and W. A. Serdijn. *Joint UWBST and IWUWBS*. May 2004. 6-10p.
7. Simon Haykin. *Communication System*. 4th Edn. John Wiley & Sons Inc (sea) Pte Ltd. 2006.
8. R. T. Hoctor and H. W. Tomlinson. *IEEE Conference on Ultra Wideband Systems and Technologies*. May 2002. 265-270.
9. Sumit Bagga, Lujun Zhang, Wouter A. Serdijn, et al. *IEEE Conference on Ultra Wide band*. September 2005. 328-332p.
10. Sumit Bagga, S. A. P. Haddad, Koen van Hartingsveldt, et al. *IEEE International Symposium of Circuits and Systems*. May 2005.
11. Mathias Johansson. *The Hilbert Transform*. Master Thesis. 06 September 2009. Mathematics/Applied Mathematics.
12. Goldberg R. R. *Fourier Transforms.* Cambridge University Press, Cambridge.
13. James E. Gilley. *Bit-Error-Rate Simulation Using Matlab*. Transcrypt International, Inc. August 19, 2003.
14. http://en.wikipedia.org/wiki/ISM_band.